Effect of a Crossflow at the Entrance to a Film-Cooling Hole

K. A. Thole[1]
Assistant Professor.

M. Gritsch
Dipl.-Ing.

A. Schulz
DR.-Ing.

S. Wittig
Professor.

Institut für Thermische Strömungsmaschinen, Universität Karlsruhe, Karlsruhe, Germany

Understanding the complex flow of jets issuing into a crossflow from an inclined hole that has a short length-to-diameter ratio is relevant for film-cooling applications on gas turbine blades. In particular, this experimental study focused on the effect of different velocities in a coflowing channel at the cooling hole entrance. Flows on both sides of the cooling hole (entrance and exit) were parallel and in the same direction. With the blowing ratio and the mainstream velocity at the hole exit remaining fixed, only the flow velocity in the channel at the hole entrance was varied. The Mach number at the hole entrance was varied between $0 < Ma_c < 0.5$, while the Mach number at the hole exit remained constant at $Ma_\infty = 0.25$. The velocity ratio and density ratio of the jet were unity giving a blowing ratio and momentum flux ratio also of unity. The single, scaled-up film-cooling hole was inclined at 30 deg with respect to the mainstream and had a hole length-to-diameter ratio of $L/D = 6$. Flowfield measurements were made inside the hole, at the hole inlet and exit, and in the near-hole region where the jet interacted with the crossflow at the hole exit. The results show that for entrance crossflow Mach numbers of $Ma_c = 0$ and 0.5, a separation region occurs on the leeward and windward side of the cooling hole entrances, respectively. As a result of this separation region, the cooling jet exits in a skewed manner with very high turbulence levels.

Introduction

Understanding the complex interaction of a jet injected into a crossflow is a phenomena of particular interest to the gas turbine industry. The primary motivation is such that by providing better blade cooling, higher turbine efficiencies can be attained by increasing turbine inlet temperatures. One such blade cooling technique is film-cooling whereby compressor bleed air is exhausted through the turbine blade surface through cooling holes. These holes typically have relatively short length-to-diameter ratios and are inclined relative to the crossflow at the jet exit. Although there are a large number of possible flow conditions at the cooling hole entrance, there have been no past film-cooling flowfield studies that have investigated the link between what is happening on the inside of the turbine blade to what is happening on the outside of the turbine blade as the film-cooling jet exits. Instead, past film-cooling studies have not considered a crossflow at the hole entrance but rather a stagnant plenum supply or very long supply tubes giving unrealistically long hole length-to-diameter ratios. The emphasis of this paper is understanding how a crossflow at the entrance of a film-cooling hole can affect the jet as it issues into a crossflow at the exit.

Understanding the effects of a crossflow at the entrance to a short hole in which the exiting flow is not yet fully developed can have implications for both numerical and experimental simulations of film-cooling. Depending upon where the film-cooling hole is located in an actual turbine blade, there are a number of different hole inlet conditions that can occur. In this study, the flow at the cooling hole entrance was considered to be parallel and in the same direction (co-flowing) to the flow at the exit of the cooling hole as would occur, for example, in the midportion of a nozzle guide vane (see Fig. 1).

The study reported in this paper is aimed at film-cooling holes for gas turbine blades where typical hole length-to-diameter ratios are short and inclined relative to the crossflow at the hole exit. Specifically, the hole length-to-diameter ratio in this investigation was an $L/D = 6$ and the inclination angle was 30 deg relative to the entrance and exit crossflows. A single, scaled-up round cooling hole with parallel crossflows at the entrance and exit of the hole was investigated. In this study, only the crossflow Mach number at the hole entrance was varied between $0 < Ma_c < 0.5$ while the Mach number at the hole exit was held constant at $Ma_\infty = 0.25$. The jet-to-mainstream velocity ratio (VR) and density ratio (DR) remained constant for all conditions at VR = 1 and DR = 1.

The following sections briefly review relevant jet-in-crossflow studies, give a description of the flow facility used for these experiments, and describe the discharge coefficient and flowfield results. After the flowfield results are discussed, there is an additional section discussing a physical description of the flow which is then followed by some conclusions.

Previous Studies

Previous studies have documented the flowfield of jet injection into a crossflow with both long (typically not used in gas turbine applications) and short jet hole lengths. These studies have encompassed a range of injection angles, and jet-to-mainstream velocity (VR) and density (DR) ratios. With the exception of the discharge coefficient study reported by Hay et al. (1983), there are no film-cooling studies in the open literature that have investigated the effect of a crossflow at the hole entrance.

Normal jet injection studies with unit density ratio (DR = 1), such as Crabb et al. (1981) and Andreopoulos and Rodi (1984), showed two obvious effects on the mean flowfield; the degree of which depended on the jet-to-mainstream velocity ratio. First, the jet was bent over by the crossflow at the exit and second the crossflow was deflected upward by the jet blockage. Both of these studies had relatively long supply holes for the jet at $L/D = 30$ for the Crabb et al. study and $L/D = 12$ for the Andreopoulos and Rodi study. Andreopoulos and Rodi found at a low velocity ratio (VR = 0.5) that the effect of the crossflow at the jet exit was to skew the exiting jet profile and force the jet to exit primarily from the downstream half of

[1] Present address: Mechanical Engineering Department, University of Wisconsin, 1513 University Avenue, Madison, WI 53706-1572.

Contributed by the Fluids Engineering Division for publication in the JOURNAL OF FLUIDS ENGINEERING. Manuscript received by the Fluids Engineering Division July 11, 1996; revised manuscript received January 29, 1997. Associate Technical Editor: L. Nelik.

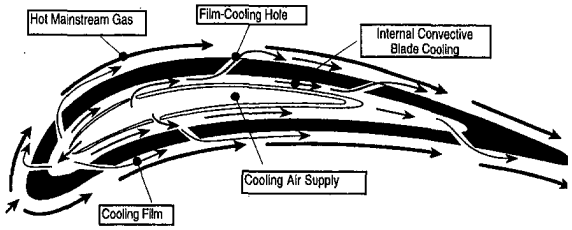

Fig. 1 Illustration of a flow configuration inside a nozzle guidevane

the hole exit plane. In fact, Andreopoulos and Rodi found at this low velocity ratio that the jet started to bend while still inside the hole passage. In contrast, at a high velocity ratio (VR = 2) they found that the jet bending occurred after the jet exited the hole passage.

Andreopoulos and Rodi also discussed that the resulting turbulence characteristics are a combination of several mechanisms. These mechanisms include the turbulence being transported to the jet hole exit from the upstream boundary layer and from inside the hole itself, turbulence being produced due to various mean velocity gradients, and turbulence being subjected to the strong streamline curvature as result of the bending jet. Andreopoulos and Rodi found at the jet centerline the location of the maximum turbulence kinetic energy and turbulent shear stress coincided with the maximum streamwise velocity gradient and concluded that the mean velocity gradient, dU/dy, was the dominant turbulent production mechanism.

Flowfield studies of inclined jet injection, with relatively short hole length-to-diameter ratios, include the experimental studies by Pietrzyk (1989), Pietrzyk et al. (1989), Subramanian et al. (1992), and numerical studies by Leylek and Zerkle (1994), Benz et al. (1993), and Garg and Gaugler (1995). Pietrzyk (1989) made flowfield measurements for an inclined jet (35 deg) subjected to a strong crossflow for jet-to-mainstream velocity ratios of VR = 0.25, 0.5, and 1 at a density ratio of DR = 1 and velocity ratios of VR = 0.25 and 0.5 at a density ratio of DR = 2. The hole length-to-diameter ratio was typical of what would be found in gas turbine applications at L/D = 3.5. The cooling hole for their configuration was supplied by a stagnant plenum. One of the dominating mechanisms hypothesized by Pietrzyk et al. (1989) was the formation of a separation region on the leeward side of the cooling hole entrance at high velocity ratios. As the jet-to-mainstream velocity ratio increased and the separation region began to form on the leeward side of the cooling hole, the jet fluid was pushed into the windward portion of the cooling hole. Hence, the primary jet exit location was shifted from the leeward side of the cooling hole at low blowing ratios, similar to Andreopoulos and Rodi (1984), to the windward side of the cooling hole. This separation region was a result of the large turning angle encountered by the coolant on the leeward side of the hole.

In addition to skewing the exiting jet profile, Pietrzyk et al. (1989) found a change in the location of the peak turbulence levels for different velocity ratio jets. At a low velocity ratio of VR = 0.25, a turbulence level of nominally Tu = 4 percent or less exited the cooling hole. As the jet interacted with the mainstream, the peak turbulence level was Tu = 12 percent which occurred at 2.5 hole diameters downstream of the jet hole center. The primary mechanism for this turbulence level was the large streamwise velocity gradient, dU/dy. At a high velocity ratio, where the formation of the separation region at the hole entrance was hypothesized, the turbulence levels exiting the cooling hole was Tu = 20 percent. This high turbulence level was equal to the peak turbulence level occurring downstream of the cooling hole due to the streamwise velocity gradient.

Leylek and Zerkle (1994) documented a full three-dimensional computational study to complement the experimental results of Pietrzyk et al. (1989). Included in their model was the supply plenum, cooling hole, and the mainstream crossflow. In the study of Leylek and Zerkle, the separation inside the jet hole was evident. Leylek and Zerkle also found that at large length-to-diameter ratios ($L/D > 3$) and high blowing ratios ($M > 1$) or small length-to-diameter ratios ($L/D < 3$) and low blowing ratios ($M < 1$), the flow inside the cooling hole became more similar to a fully developed turbulent pipe flow. Benz et al. (1993) also realized the importance of simulating the flow inside the jet hole as they prescribed a uniform velocity profile at the cooling hole entrance that resulted in a skewed jet exit profile for a film-cooling hole in the leading edge region of a turbine blade.

As mentioned earlier, Hay et al. (1983) studied the effects of jet entrance and exit crossflows on the discharge coefficients of film-cooling holes. Being able to predict the discharge coefficients is critical in the sizing of film-cooling holes since an excess of unnecessary coolant fluid represents a loss in the turbine working fluid. Hay, et al. investigated a range of Mach number crossflows at the inlet and exit of their cooling hole, hole inclination angles, and hole length-to-diameter ratios. They found that the crossflow at the jet entrance had a stronger effect on the discharge coefficient relative to the effect of the crossflow at the hole exit. For example, in the case where the crossflow at the hole entrance, which was parallel and in the same direction as the flow at the hole exit, increased from $Ma_c = 0$ to $Ma_c = 0.4$, the discharge coefficient increased by 30 percent. In contrast, as the exit Mach flow increased from $Ma_\infty = 0$ to $Ma_\infty = 0.5$, the discharge coefficient decreased by only 10 percent

Nomenclature

C_D = discharge coefficient = actual mass flowrate/ideal mass flowrate
D = cooling hole diameter
DR = jet-to-mainstream density ratio
L = cooling hole length measured along the centerline axis
M = jet-to-mainstream blowing or mass flux ratio, $M = \rho_j V_j / \rho_\infty V_\infty$
Ma_c = Mach number of the crossflow at the jet hole entrance
Ma_∞ = Mach number of the crossflow at the jet hole exit
$P_{t,c}$ = stagnation pressure at hole entrance
p_∞ = static pressure at the hole exit
Re_D = Reynolds number based on hole diameter
Re_θ = Reynolds number based on momentum thickness
Tu = turbulence intensity (percent)
u', v' = streamwise and vertical rms velocities
U, V = streamwise and vertical mean velocity components
V_j = total jet velocity based on inlet hole diameter and mass flux
VR = jet-to-mainstream velocity ratio
x = streamwise distance measured from the cooling hole centerline
y = vertical distance measured from the top of the cooling hole
y_c = vertical distance measured from the bottom of the coolant channel
z = spanwise distance measured from the cooling hole centerline
δ_{99} = boundary layer thickness, 99 percent point
θ = momentum thickness
ρ = density

Subscripts and Superscripts

c = crossflow conditions at the hole entrance
∞ = crossflow conditions at the hole exit

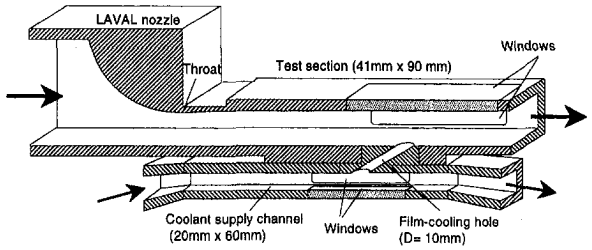

Fig. 2 Schematic of the test rig showing the primary channel at the cooling hole exit and the supply channel at the cooling hole entrance

for pressure ratios of $1.05 < P_{t,c}/p_\infty < 1.4$ and remained constant when the pressure ratios were $P_{t,c}/p_\infty > 1.4$.

The exiting velocity profile can, in fact, have a significant impact on the heat transfer occurring downstream of the film-cooling hole. The importance of the exiting jet profile on surface heat transfer is critical and best described by Garg and Gaugler's (1995) study. The numerical results presented by Garg and Gaugler (1995) showed large differences in surface heat transfer depending upon the exiting jet velocity and temperature profiles for several film-cooled turbine blades. Garg and Gaugler presented heat transfer predictions that had differences by as much as 50–60 percent depending upon whether a parabolic or one-seventh jet profile was assumed to exit the cooling hole. In addition, Schmidt et al. (1996) presented a discussion on the hole length-to-diameter effects which, in fact, causes differing exiting jet profiles. In comparing their data, which had an $L/D = 4$, to the data of Sinha et al. (1991), which had an $L/D = 1.75$, a clear detachment and reattachment of the jet from the downstream surface occurred for the shorter $L/D = 1.75$, but not for the longer $L/D = 4$.

These experimental and numerical results illustrate the importance of understanding the formation of the jet inside the cooling hole before the jet exits into the mainstream crossflow. A skewed exiting jet profile increases the penetration of the jet since there is a higher effective velocity in some locations at the jet exit. An increased penetration of the jet can cause a detachment of the jet from the downstream blade surface. This jet detachment has a large penalty in turbine blade cooling. In addition to a skewed jet profile, the separation region occurring at the hole inlet produces relatively high turbulence levels for the exiting jet. These high turbulence levels will increase the coolant fluid diffusion and reduce the thermal protection of the blade.

To evaluate how the entrance condition ultimately affects the film-cooling flowfield, the facility used for these experiments included a channel at the film-cooling hole entrance and exit, which could provide either a plenum condition or crossflow condition. The channel at the hole entrance represents the internal core of a nozzle guide vane while the channel at the hole exit represents the external flow around the nozzle guide vane. In the study presented here, the hole geometry as well as the supply channel geometry was based on a consensus of European gas turbine companies. The following section describes the experimental facility used for these experiments.

Experimental Facility

The experiments discussed in this paper were conducted in a test facility at the Institut für Thermische Strömungsmaschinen (ITS), Universität Karlsruhe. This facility is described in detail by Wittig et al. (1996) with previous shaped film-cooling hole studies, also conducted in this facility, reported by Thole et al. (1996). A sketch of the test section, which contained the single, scaled-up film-cooling hole is shown in Fig. 2. The jet hole entrance and exit crossflow channels were controlled independently, which allowed the effect of the entrance Mach number crossflows to be studied.

Table 1 Flow conditions for exit and entrance crossflow conditions

	Exit crossflow conditions	Entrance crossflow conditions
Mach number	0.25	0, 0.30, and 0.5
Mean freestream velocity (m/s)	85.0	0, 102.7, and 168.0
Freestream turbulence intensity (%)	2	1
Total temperature at injection (K)	300	300
ReD	5.2×10^4	6.6×10^4
δ_{99}/D at $x/D = -5$	0.8	
Reθ at $x/D = -5$	3000	
δ_{99}/D at $x/D = -7$		0.2

The primary channel at the jet exit was 90 mm in width and 41 mm in height while the supply channel at the jet entrance was 60 mm in width and 20 mm in height. The hole diameter for these experiments was 10 mm and was machined into a flat aluminum test plate that was 30 mm thick. For these studies, the holes were machined to have sharp corners which, in fact, may not be representative of an actual turbine blade depending on the manufacturing procedure used. The round hole was inclined at 30 deg giving a hole length-to-diameter ratio of $L/D = 6$. The flow conditions in the primary and supply channels are given in Table 1. The jet-to-mainstream velocity ratio and density ratio were constant at VR = 1 and DR = 1 for all of the flowfield results presented in this paper.

The air for both flow channels was supplied by a large compressor that has a capacity of producing 1 kg/s at 11 Bars. Flow for the coolant channel was also provided by the compressor, but driven by a sealed external blower in the supply flow loop. The turbulence levels at both the entrance and exit to the cooling hole were a result of those naturally occurring in both of the flow loops.

The flowrate in the supply channel was varied to give the different Mach numbers at the hole entrance. For the $Ma_c = 0.3$ case, the mass flowrate in the supply channel was 0.12 kg/s. In contrast, for each of the three channel conditions studied the flowrate through the cooling hole was fixed at 7.5e−03 kg/s giving a velocity ratio of VR = 1. Fixing this mass flowrate was achieved by adding the 7.5e−03 kg/s to the supply channel which was then ejected from the hole. To reduce the uncertainty, the mass flowrate through jet hole was determined by measuring this mass flowrate entering the secondary supply channel. Leak tests were conducted on the secondary supply channel to insure that all of the mass flowrate entering the supply channel was exhausted only through the cooling hole. The discharge coefficients, pressure ratios, and stagnation and static pressure ratios for all three flow entrance crossflow conditions are shown in Table 2. Note that the high velocity condition in the channel ($Ma_c = 0.5$) may be undesirably high for internal flows in an actual turbine vane, but was studied to better understand the hole entrance effects. In addition, the crossflow velocity that is present at the hole entrance depends on a number of design considerations.

The inlet flow conditions for both the jet entrance and exit channel flows are shown in Fig. 3. The boundary layer profile

Table 2 Flow conditions for the three entrance crossflow conditions

	Stagnation pressure, $P_{t,c}$ (mbars)	Hole exit static pressure p_∞ (mbars)	Pressure ratio, $P_{t,c}/p_\infty$	Discharge coefficient, C_d
$Ma_c = 0.0$	1097.5	996.6	1.10	0.72
$Ma_c = 0.3$	1086.4	996.9	1.09	0.72
$Ma_c = 0.5$	1176.0	996.2	1.18	0.47

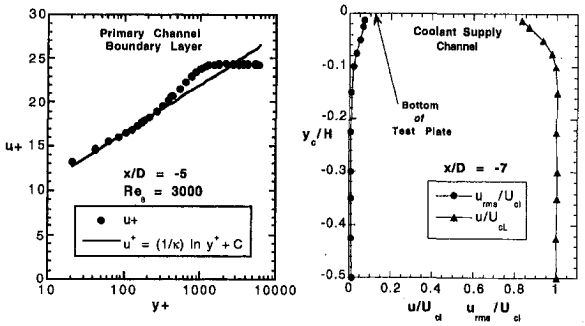

Fig. 3 Inlet flow conditions for the primary channel and for the supply channel

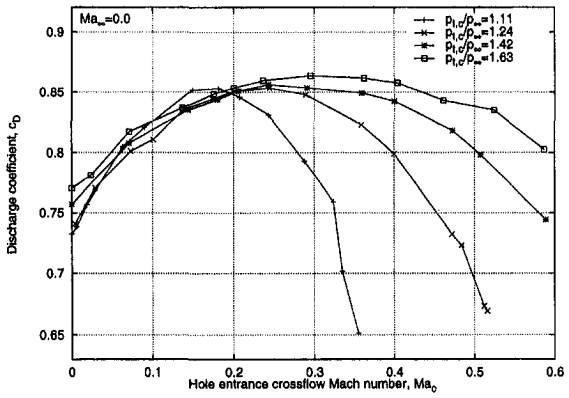

Fig. 4 Discharge coefficient measurements for a range of entrance crossflow Mach numbers (Ma$_c$) and no exit crossflow (Ma$_\infty$ = 0)

measured in the primary channel (at the jet exit) was measured five hole diameters upstream of the hole centerline. The coolant supply channel (at the jet hole entrance) was measured seven hole diameters upstream of the hole centerline. As illustrated in Fig. 3, the bottom of the test plate refers to the inlet to the coolant hole. The supply channel flow was considered to be a boundary layer flow with a thickness of $\delta_{99} \approx 2$ mm ($y_c/H = -0.1$) as compared to a channel half-height of 10 mm at a location of seven hole diameters upstream of the hole inlet.

A two-component, coincident, fiber optic laser Doppler velocimeter (LDV) was used to measure velocity fields for the three flow cases. The commercial Dantec LDV system had an 85 mm fiber optic probe and Enhanced Burst Spectrum Analyzers. A beam expander reduced the probe volume size to a diameter of 74 μm and a length of 0.6 mm. The data was bias corrected using residence time weighting. Both the primary and supply channel flows were seeded with oil (DES) particles having a mean diameter of 0.5 μm. Because the supply channel and primary flow were at different pressures, valves were used downstream of the seeder such that the seeding injection was independently controlled to avoid velocity biases.

The test section in the mainstream channel had glass on both side walls and top walls which allowed for optical access. The LDV was positioned on the side of the test section to measure the streamwise and vertical velocity components and was positioned on the top of the test section to measure the streamwise velocity components inside the jet hole. When positioned on the side of the test section, the LDV was rotated at 45 deg and tilted at nominally 4.5 deg to allow near-wall measurements. As a result of the tilt, the vertical velocity, v, reported in this paper contains a small lateral velocity component. Similarly when the LDV was positioned on the top of the test section, a 7 deg tilt was needed to avoid severe surface reflections. In both measurement configurations, however, the tilt has no affect on the streamwise velocity component.

Uncertainty Estimates

Based on a 95 percent confidence interval, both bias and precision uncertainties were quantified. The data presented in this paper were typically averaged over 10,000 points or more depending on the data rate. The bias uncertainty for the mean velocities were 0.4 percent whereas the precision uncertainties were one percent in the freestream and 3.4 percent near the wall. The precision uncertainty for the rms velocity measurements were 1.4 percent in the freestream and 5.8 percent near the wall. The precision uncertainty in the turbulent shear stress was 5.6 percent. Positioning the LDV probe volume with respect to the hole was $\Delta x = \pm 0.05$ mm, $\Delta y = \pm 0.05$ mm, and $\Delta z = \pm 0.05$ mm. The uncertainty in setting the coolant mass flowrate was two percent and the overall uncertainty in the discharge coefficient was four percent.

Discharge Coefficient Measurements

Discharge coefficients were measured for a number of conditions. Figure 4 shows the variation of the discharge coefficients as a function of the crossflow at the hole entrance alone. Note that for the data presented in Fig. 4, there is no crossflow at the hole exit.

The four curves represent different ratios of total coolant (at jet hole entrance) to static (at jet hole exit) pressure ($P_{t,c}/p_\infty$) ratios between $1.11 < P_{t,c}/p_\infty < 1.63$. Similar to the results presented by Hay et al. (1983) who investigated a $P_{t,c}/p_\infty$ ratio greater than 1.6, as the entrance crossflow Mach number increases to Ma$_c$ = 0.4, so does the discharge coefficient. However, at $P_{t,c}/p_\infty = 1.63$ there is a decrease in the discharge coefficient as the crossflow Mach number at the inlet increases beyond Ma$_c$ = 0.4. This increase in the discharge coefficient followed by a decrease occurs for all pressure ratios. Although the maximum discharge coefficient for all the pressure ratios investigated is between $C_d = 0.85$ and 0.86, the Ma$_c$ at which this maximum occurs decreases as the $P_{t,c}/p_\infty$ ratio decreases. For the lowest pressure ratio, $P_{t,c}/p_\infty = 1.11$, the maximum occurs at a Ma$_c$ = 0.18 while at the highest pressure ratio, $P_{t,c}/p_\infty = 1.63$, the maximum occurs at Ma$_c$ = 0.3. The data also indicate that as the pressure ratio across the hole increases, the Ma$_c$ range over which the discharge coefficient is a maximum increases. Gritsch et al. (1997) show that the same trends occur even when there is a crossflow up to a Ma$_\infty$ = 0.6 at the exit of the hole.

Hay et al. (1983) attributed the increased discharge coefficient to the additional dynamic head. Figure 4 clearly indicates that there is an additional effect occurring as the inlet crossflow Mach number is increased beyond the condition of the maximum discharge coefficient. This effect will be clarified in the following sections of this paper which describe the flowfield measurements. It is clear, however, that the crossflow at the hole entrance plays a key role in the discharge coefficient for that jet hole at all pressure ratios.

Flowfield Results

Although flowfield measurements have previously been reported for round film-cooling holes with a crossflow at the jet exit, as mentioned in the introduction, there have not been any studies which have investigated the effect of a crossflow at the jet entrance. The following sections present the mean flowfield results and turbulent flowfield characteristics for single, scaled-up round jet hole all at a velocity ratio of VR = 1. The three cases presented are for jet entrance crossflow Mach numbers at Ma$_c$ = 0, 0.3, and 0.5. The jet exit crossflow Mach number remained constant for all of the flowfield tests at Ma$_\infty$ = 0.25.

The turbulent flowfield measurements are presented in terms of turbulence levels which use the measured rms velocities

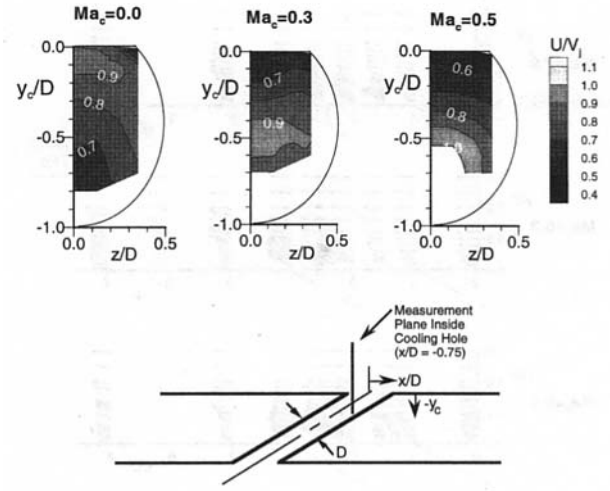

Fig. 5 Mean streamwise velocity contours inside the jet hole at $x/D = -0.75$ for entrance crossflows of $Ma_c = 0$, 0.3, and 0.5

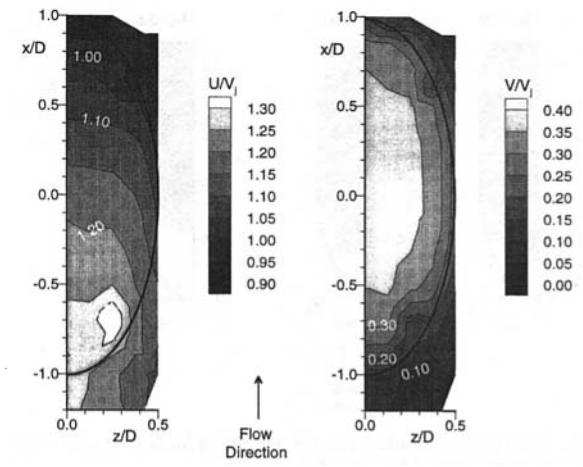

Fig. 6 Mean streamwise and vertical velocity contours at the entrance to the jet hole at $y_c/D = -0.15$ with a crossflow at the hole entrance of $Ma_c = 0.3$

referenced with the relevant mean velocity rather than the local mean velocity. For the turbulence levels presented inside and just at the jet hole exit plane, the streamwise rms velocities are used and normalized by the average jet velocity, Tu_j (percent) $= 100 \times \sqrt{u'^2}/V_j$, whereas the turbulence levels presented after the jet has exited into the crossflow, the streamwise and vertical rms velocities are normalized by the mean mainstream velocity, Tu (percent) $= 100 \times \sqrt{0.5(u'^2 + v'^2)}/U_\infty$. Since these tests were conducted at a VR = 1, both the mean mainstream and average jet velocities are the same.

Flowfield Inside Jet Hole. To fully understand the jet profile at the hole exit, measurements were made inside the jet hole passage as shown by the measurement plane in Fig. 5. The mean streamwise velocity component inside the jet hole were measured by placing the LDV above the jet hole. Reflection effects were minimized by putting a slight tilt on the LDV and by painting the inside surface of the hole with a velvet black paint. The measurements were taken in a vertical-spanwise plane at a streamwise distance of $x/D = -0.75$ upstream of the hole centerline or just 0.25 hole diameters downstream of the windward edge of the cooling hole. This location was chosen because it was the farthest upstream position that still allowed the LDV beams to cross as they entered into the cooling hole.

The streamwise mean velocity contours inside the cooling hole for the three different entrance crossflow Mach numbers ($Ma_c = 0$, 0.3, and 0.5) are shown in Figure 5. The streamwise velocity contours are normalized by the total jet velocity. As indicated by the figures, the position at which the highest contour level occurs depends strongly upon the entrance crossflow Mach number. For the plenum-type supply ($Ma_c = 0$), a large portion of the jet (highest streamwise velocity contour) is at the top portion of the cooling hole. This placement of the jet is consistent with previous studies (Leylek and Zerkle, 1994). The previous computational study by Leylek and Zerkle has shown that when there is no crossflow at the hole entrance, i.e., a stagnant plenum, the jet inside the hole is pushed towards the windward edge of the hole because of the separation region on the leeward entrance to the hole. These experiments confirm that in fact the jet has been pushed toward the windward side which would appear at the top of the vertical-spanwise plane at $x/D = -0.75$.

As the cross-flow Mach number is increased at the hole entrance, the position of the maximum streamwise velocity contour shifts toward the leeward side of the cooling hole. Where the entrance crossflow Mach number is $Ma_c = 0.3$, the maximum streamwise velocity is located primarily in the center of the hole ($y/D = -0.5$). There is only a slight shift toward the leeward side (bottom) of the cooling hole for the higher crossflow entrance Mach number, $Ma_c = 0.5$. Figure 6 shows the total velocity contours (based on the streamwise and vertical velocity components) at the hole entrance of the jet for the $Ma_c = 0.3$ crossflow condition. These measurements were taken at $y_c/D = -0.15$ which is downward into the supply channel measured at the entrance of the cooling hole. Figure 6 indicates that a large portion of the jet is entering in the center of the cooling hole.

The turbulence levels inside the jet holes (based on the rms of the streamwise velocity fluctuations and the mean freestream velocity) are quite different for the three different entry Mach number crossflows. Figure 7 shows a comparison of those turbulence level contours. Very high turbulence levels occur for both the low and high entry crossflow conditions ($Ma_c = 0$ and 0.5). The peak turbulence levels for these two cases are nominally Tu = 17 percent. The turbulence levels for the condition in which the entry and exit crossflow Mach numbers are matched $Ma_c = 0.3$ is much lower with a peak at Tu = 10.5 percent. It is clear that for the portion of the hole that was mapped, most of the hole has overall lower turbulence levels for the $Ma_c = 0.3$ case. High turbulence levels exiting the hole for film-cooling applications can have a detrimental effect in that the jet fluid will tend to mix with the "hot" mainstream fluid more rapidly and not be as effective in cooling the blade surface.

Flowfield at the Jet Exit. The total velocity contours (based on the mean streamwise and vertical velocity components), measured in a streamwise-spanwise plane just at the exit of the hole ($y/D = 0.1$), are shown in Figs. 8. Depending upon the development of the jet inside of the cooling hole, there are countervening effects between the crossflow at the jet exit, which tends to bend the jet, and the jet velocity profile itself,

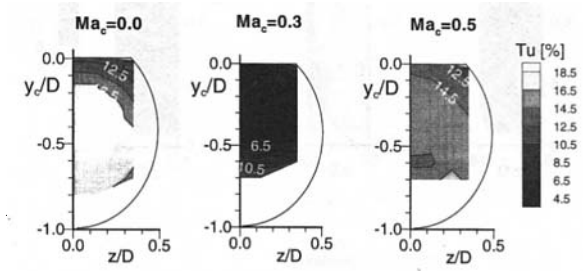

Fig. 7 Turbulence level contours inside the jet hole at $x/D = -0.75$ for entrance crossflows of $Ma_c = 0$, 0.3, and 0.5

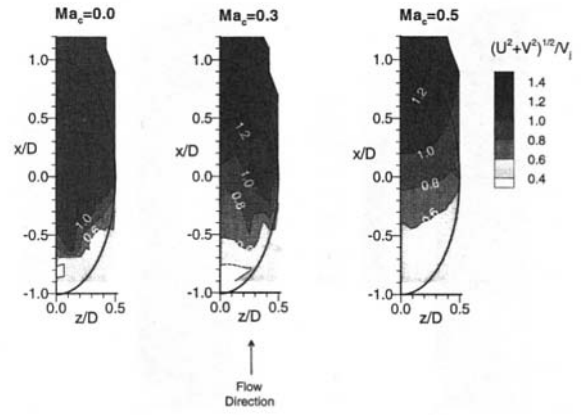

Fig. 8 Total velocity contours at the exit of the jet hole at y/D = 0.1 for entrance crossflows of Ma$_c$ = 0, 0.3, and 0.5

which may have a higher momentum in particular regions due to the skewed velocity profile.

As shown in the previous section for the low Mach number crossflow at the hole entrance, Ma$_c$ = 0, a large portion of the jet is located in the windward side of the cooling hole. The skewing of jet profile for the Ma$_c$ = 0 case would be such that the jet flow is able to counteract the mainstream crossflow at the jet exit. In fact, the jet exit location begins near the windward side of the cooling hole. At a Ma$_c$ = 0.3, the jet exit moves more towards the leeward side of the cooling hole and at a Ma$_c$ = 0.5, the jet exit is even more near the leeward side of the cooling hole at relatively high velocities. The skewing of the jet as it exits the cooling hole causes a higher penetration into the crossflow at the exit of the hole (as will be shown in the next section).

The turbulence levels (based on the streamwise and vertical velocity components and the mean freestream velocity) at the jet exit, shown in Fig. 9, are similar to those seen inside the jet hole. Note that there is a change in the scale used for the turbulence level contours as compared to the scale that was used in Fig. 7. Very high turbulence levels occur for the Ma$_c$ = 0 and 0.5 cases whereas for the Ma$_c$ = 0.3 case the turbulence levels are much lower. The peak turbulence level exiting those cooling holes is Tu = 16 percent and Tu = 21 percent for the Ma$_c$ = 0 and Ma$_c$ = 0.5 cases, respectively. The peak turbulence level exiting the hole for the Ma$_c$ = 0.3 case is lower at Tu = 11 percent.

Flowfield in the Mainstream Crossflow. The mean streamwise-vertical velocity vectors, measured at the jet centerline in the streamwise-vertical plane, are shown in Fig. 10. As

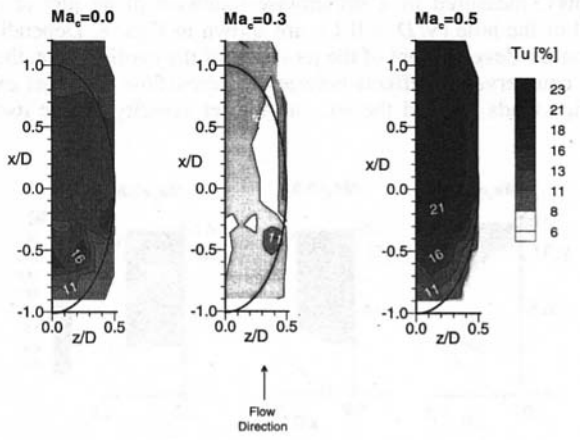

Fig. 9 Turbulence level contours at the exit of the jet hole at y/D = 0.1 for entrance crossflows of Ma$_c$ = 0, 0.3, and 0.5

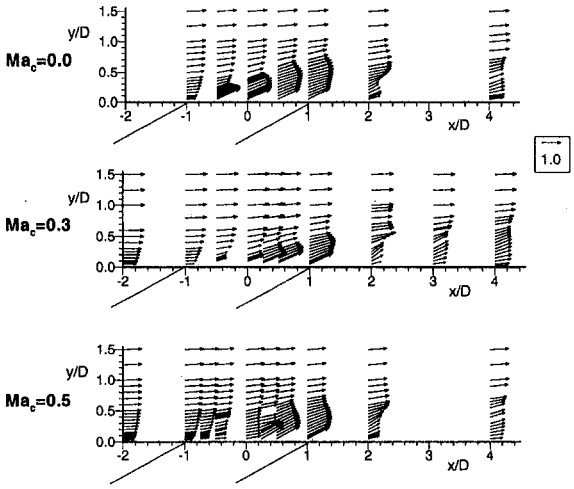

Fig. 10 Mean velocity vectors in the exit crossflow at the hole centerline (z/D = 0) for entrance crossflows of Ma$_c$ = 0, 0.3, and 0.5

expected from the previous discussion, the Ma$_c$ = 0 case shows a strong vertical jet penetration which begins near the upstream edge of the cooling hole. In comparison, the Ma$_c$ = 0.5 crossflow at the entrance causes the jet to exit from the leeward side of the cooling hole.

Figure 11 shows the streamwise and vertical velocity profiles in the near-hole region at the jet centerline at x/D = 0 and 1. These figures clearly show that for no crossflow at the hole entrance (Ma$_c$ = 0) the jet has exited the cooling hole x/D = 0. At the downstream edge of the jet hole, x/D = 1, the Ma$_c$ = 0.5 case shows higher streamwise and vertical velocity components indicating the exit location near the leeward side of the hole.

The turbulence level contours, measured at the jet centerline in a streamwise-vertical plane, are shown in Fig. 12. As discussed in the previous section the turbulence levels exiting the hole are significantly higher for the Ma$_c$ = 0 and Ma$_c$ = 0.5 entrance conditions. In addition, large mean streamwise velocity gradients for the Ma$_c$ = 0 and Ma$_c$ = 0.5 entrance conditions are causing higher peak turbulence levels after the jet has exited the cooling hole in comparison to the Ma$_c$ = 0.3 case. The peak turbulence levels, which occur at x/D = 2, are Tu = 28 percent for the Ma$_c$ = 0 case and Tu = 36 percent for the Ma$_c$ = 0.5 case. In contrast, at x/D = 2 the peak turbulence level for the Ma$_c$ = 0.3 case was Tu = 16 percent.

Physical Description of Entrance Crossflow Effects

The previous sections describe the flowfield differences occurring when a crossflow is present at the entrance to a represen-

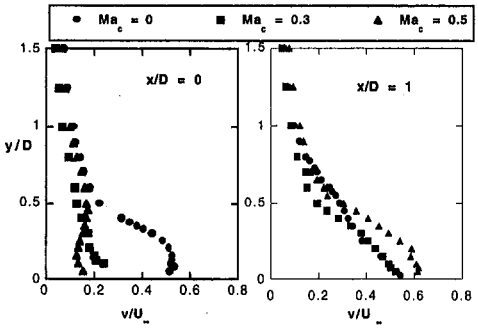

Fig. 11 Comparison of the streamwise and vertical velocity components in the near-hole region at the hole centerline (z/D = 0) for entrance crossflows of Ma$_c$ = 0, 0.3, and 0.5

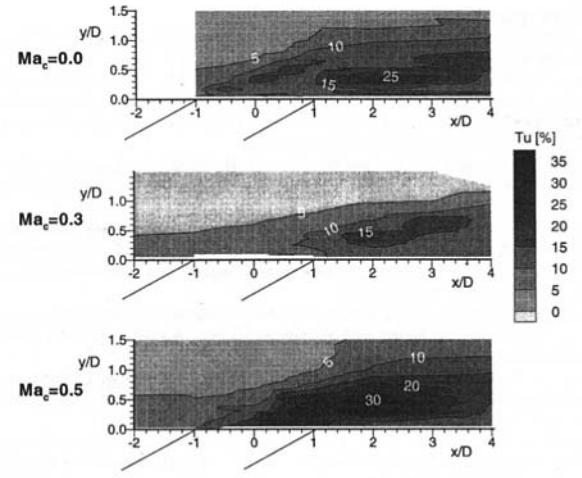

Fig. 12 Turbulence level contours in the exit crossflow at the hole centerline ($z/D = 0$) for entrance crossflows of $Ma_c = 0$, 0.3, and 0.5

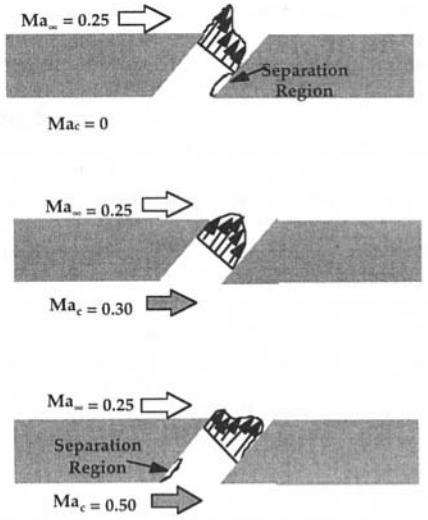

Fig. 13 Physical interpretation of the effects that a crossflow at the jet hole entrance has on the jet flowfield

tative film cooling hole as it exits into a crossflow. This section gives a physical description of this jet flow.

At a velocity ratio of VR = 1 with no crossflow at the hole entrance, previous studies have shown that a separation region occurs on the leeward side of the hole entrance (Pietrzyk et al., 1989 and Leylek and Zerkle, 1994). These previous studies have shown that there are a number of effects that result from this separation region. First, the exiting profile is skewed causing more jet fluid to exit from the windward side of the jet hole. This skewed profile causes a higher penetration distance of the jet into the mainstream. As was discussed in the introduction, when the separation region occurs on the leeward side of a short L/D hole in which the skewness of the profile would be more prominent than for a long L/D hole where the velocity profile had more time to readjust from the separation, adiabatic effectiveness measurements indicated the cooling jet detaches and then reattaches to the downstream surface (Schmidt, et al., 1996). Second, the exiting jet has very high turbulence levels which promotes a more rapid mixing with the hot mainstream. The data presented in this paper concurs that when there is no crossflow at the entrance to the jet hole ($Ma_c = 0$) a large portion of the jet exits from the windward side of the hole having turbulence levels higher than would occur say, for example, a pipe flow.

Pietrzyk (1989) presents a good description of the shear layers occurring due to the cooling jet/mainstream interaction at low and high velocity ratios. The shear gradients are particularly relevant since the dU/dy gradients at the jet centerline are responsible for the turbulence production. At velocity ratios greater than VR > 0.5, he shows a windward shear layer that occurs at the interface between the mainstream and the cooling jet as the jet exits the hole; a wake region behind the jet which is formed due to the jet blockage; and a wall-jet layer formed downstream of the wake region near the wall. Pietrzyk (1989) pointed out that the highest turbulence production occurs in the windward shear layer, or rather the interface between the jet and the mainstream, and is primarily a result of the large dU/dy velocity gradients. Similarly in this paper for the case with no crossflow entrance to the jet hole ($Ma_c = 0$), the peak turbulence levels occurred at an $x/D = 2$ where the most intense dU/dy velocity gradients occurred.

For the cases presented in this paper in which a strong crossflow existed, the $Ma_c = 0.5$ crossflow also showed elevated turbulence levels exiting from the cooling hole, similar to the case with no crossflow at the hole entrance. However, the jet profile exiting from the cooling hole is much different in that a large portion of the jet is skewed towards the leeward side of the cooling hole. In the highest entrance crossflow case, there are even higher dU/dy velocity gradients because the higher jet velocities are interacting with the low-speed fluid near the wall. As a result, turbulence levels even higher than those for the no crossflow case ($Ma_c = 0$) occur. For the case where the entrance crossflow is $Ma_c = 0.3$, the turbulence levels are significantly lower exiting the hole and the velocity profile indicates that the jet exits more towards the middle portion of the hole. This more uniform jet profile then reduces the velocity gradient and, subsequently, the turbulence production.

As the Mach number increases at the entrance to the jet hole from $Ma_c = 0$ to $Ma_c = 0.5$, the separation region which forms changes from the leeward side of the jet to the windward side of the jet hole. This effect is shown schematically in Figure 13. Since the turbulence levels are fairly low and the jet profile inside the hole appears to be more symmetric for the $Ma_c = 0.3$ entrance crossflow, the effect of the separation region, if there is a separation region, is not very large. In the $Ma_c = 0$ case, the downstream fluid has a large turning angle to overcome which causes the separation on the leeward side of the hole entrance. In the $Ma_c = 0.5$ case, the upstream fluid has an effectively large turning angle to overcome which causes a separation on the windward side of the hole entrance. Consistent with those separation regions are that both the $Ma_c = 0$ and $Ma_c = 0.5$ cases have high turbulence levels occurring inside the hole.

The discharge coefficients which were presented showed the entrance crossflow effect alone. Those results indicated that there was an entrance crossflow condition in which the discharge coefficient was a maximum. Below a $Ma_c < 0.15$, all of the pressure ratio cases indicated increases in discharge coefficients as the Ma_c increased. The increase in the discharge coefficient with increasing Ma_c occurs because the separation region on the leeward side of the hole passage begins to become minimal. For the low pressure ratio case of $P_{t,c}/p_\infty = 1.11$, the discharge coefficient begins to rapidly decrease at a $Ma_c = 0.2$ indicating that the total pressure is not high enough to overcome the frictional and separation losses. For the high pressure ratio case $P_{t,c}/p_\infty = 1.63$, the additional total pressure is enough to overcome the losses for a larger Ma_c range.

Conclusions

The results presented in this paper indicate the importance of understanding not only the effects of the crossflow at the jet exit, but also flowfield effects at the jet hole entrance. The flowfields for a round, inclined hole having a short length-to-

diameter ratio in which the jet is exposed to a crossflow at the hole entrance have not been reported in the open literature prior to this investigation. These types of flows commonly occur as film-cooling holes on gas turbine blades and, in particular, a crossflow at the hole entrance occurs for nozzle guide vanes. With improvements and changes to inner blade convective cooling schemes, an understanding as to how a crossflow at the hole entrance can influence the exiting jet profile and the discharge coefficients (hole sizing) is needed.

The mean velocity field measurements show that when the jet has no crossflow at the hole entrance, there is a separation region on the leeward side of the hole entrance which causes the jet to exit from the upstream portion of the hole. Alternatively, when there is a high velocity crossflow at the hole entrance, there is a separation region on the windward side of the hole entrance which causes the jet to exit from the downstream portion of the hole. These skewed profiles lead to higher turbulence production after the jet interacts with the mainstream.

In addition to a skewing of the jet as it exits the hole, increased turbulence levels inside the cooling hole and reduced discharge coefficients occur because of this separation region. As turbulence levels increase, the jet fluid would have a tendency to mix quickly with the mainstream at the jet exit. From a gas turbine film-cooling standpoint, this effect is detrimental because of the decreased cooling capability.

Acknowledgments

This study was partly funded by the European Union through grant by the Brite Euram program "Investigation of the Aerodynamics and Cooling of Advanced Engine Turbine Components" under Contract AER2-CT92-0044. The authors wish to express their gratitude to the partners involved in the program for the permission to publish this paper and to R. Clifford from Rolls-Royce, who played an active role in initiating and coordinating the work program.

References

Andreopoulos, J. and Rodi, W., 1984, "Experimental Investigation of Jets in a Crossflow," *Journal of Fluid Mechanics,* Vol. 138, pp. 93–127.

Benz, E. Wittig, S., Beeck, A., and Fottner, L., 1993, "Analysis of Cooling Jets near the Leading Edge of Turbine Blades," 72nd Fluid Dynamics Panel Meeting and Symposium on *Computational and Experimental Assessment of Jets in Cross Flow,* Winchester, UK, Paper no. 37.

Crabb, D., Durao, D. F. G., and Whitelaw, J. H., 1981, "A Round Jet Normal to a Crossflow," ASME JOURNAL OF FLUIDS ENGINEERING, Vol. 103, pp. 143–153.

Garg, V. K. and Gaugler, R. E., 1995, "Effect of Velocity and Temperature Distribution at the Hole Exit on Film Cooling of Turbine Blades," presented at the International Gas Turbine and Aeroengine Congress and Exposition, Houston Texas, ASME Paper No. 95-GT-2.

Gritsch, M. Schulz, A. and Wittig, S., 1997, "Discharge Coefficient Measurements of Film-Cooling Holes with Expanded Exits," ASME Paper No. 97-GT-165, Orlando, Florida.

Hay, N., Lampard, D., and Benmansour, S., 1983, "Effect of Crossflows on the Discharge Coefficient of Film Cooling Holes," ASME *Journal of Engineering for Power,* Vol. 105, pp. 243–248.

Leylek, J. H. and Zerkle, R. D., 1994, "Discrete-Jet Film Cooling: A Comparison of Computational Results with Experiments," ASME *Journal of Turbomachinery,* Vol. 116, pp. 358–368.

Pietrzyk, J. R., Bogard, D. G., and Crawford, M. E., 1989, "Hydrodynamic Measurements of Jets in Crossflow for Gas Turbine Film Cooling Application," ASME *Journal of Turbomachinery,* Vol. 111, pp. 1139–145.

Pietrzyk, J. R., 1989, "Experimental Study of the Interaction of Dense Jets with a Crossflow for Gas Turbine Applications," Ph.D. dissertation, University of Texas at Austin.

Schmidt, D. L., Sen, B., and Bogard, D. G. 1996, "Film Cooling with Compound Angle Holes: Heat Transfer," ASME *Journal of Turbomachinery,* Vol. 118, pp. 800–806.

Sinha, A. K., Bogard, D. G., Crawford, M. E., 1991, "Film Cooling Effectiveness Downstream of a Single Row of Holes with Variable Density Ratio," ASME *Journal of Turbomachinery,* Vol. 113, pp. 442–449.

Subramanian, C. S., Ligrani, P. M., Green, J. G., Doner, W. D., and Kaisuwan, P., 1992, "Development and Structure of a Film-Cooling Jet in a Turbulent Boundary Layer with Heat Transfer," *Rotating Machinery Transport Phenomena, Proceedings of the Third International Symposium on Transport Phenomena and Dynamics of Rotating Machinery* (ISROMAC-3), pp. 53–68.

Thole, K. A., Gritsch, M., Schulz, A., and Wittig, S., 1996, "Flowfield Measurements for Cooling Holes with Expanded Exits," ASME Paper No. 96-GT-174, Birmingham England.

Wittig, S., Schulz, A., Gritsch, M., and Thole, K. A., 1996, "Transonic Film Cooling Investigations: Effects of Hole Shapes and Orientations," ASME Paper No. 96-GT-222, Birmingham England.